

Toward Stabilization of Domains in Polymer Bulk Heterojunction Films

Bobak Gholamkhash and Steven Holdcroft*

Department of Chemistry, Simon Fraser University, 8888 University Drive, Burnaby, BC, V5A1S6, Canada

Received June 30, 2010. Revised Manuscript Received August 22, 2010

With the purpose of studying the effect of stabilizing film morphology on polymer photovoltaic cell performance, the morphology and characteristics of bulk heterojunction devices fabricated using binary blends of an azide-functionalized graft copolymer of poly(3-hexylthiophene) (P3HT) and [6,6]-phenyl C₆₁-butyric acid methyl ester (PCBM) were examined. A thermal, solid state reaction between the azide groups attached to P3HT and PCBM, confirmed by Fourier transform infrared spectroscopy (FTIR) and UV–vis spectroscopies, rendered the films largely insoluble and stabilized the morphology, as evidenced by limited growth of macroscopic crystals of PCBM over time, although transmission electron microscopy (TEM) analysis revealed no dramatic changes in morphology at the nanoscopic level. Photovoltaic (PV) devices prepared from these stabilized layers exhibited 1.85% power conversion efficiencies (PCE) which fell to 0.93% over 3 h at 150 °C, whereas native P3HT/PCBM devices, initially displaying 2.5% PCE dropped to 0.5% over the same period. The extent to which the morphology of the bulk heterojunction can be stabilized by this route is discussed.

Introduction

Organic electronic devices based on conjugated polymers have drawn considerable attention as a result of their potential in the fabrication of low cost, large-area devices on flexible substrates.^{1,2} An area of recent activity is solution processing of photovoltaic (PV) cells. Here, conjugated polymers, in combination with molecular electron acceptors, are capable of reaching solar power conversion efficiencies in excess of 5%^{2c} and, most recently, as high as 7.4% for a low band gap polymer based on alternating thieno[3,4-b]thiophene and benzodithiophene units,^{2g} as well as poly(2,5-thienylene vinylene) derivatives^{2h} for all of which formation of ordered structures are the prominent feature.

Blends of poly(3-hexylthiophene) (P3HT) and [6,6]-phenyl C₆₁-butyric acid methyl ester (PCBM) are considered the technological benchmark against which state-of-the-art

organic photovoltaics are measured.² In these systems, the electron-donating polymer and electron-accepting fullerene form a nanometer-sized interpenetrating network, commonly termed as a donor–acceptor (D–A) bulk heterojunction (BHJ). At the D–A interface, excitons dissociate into free charge carriers and the bicontinuous D–A network provides separate pathways for effective transportation of the charges, i.e., holes and electrons, to the electrodes. The three-dimensional nanomorphology of the active layer provides a large interfacial area and facilitates efficient exciton dissociation. In principle, the size of the donor and acceptor domains should be comparable to the exciton diffusion length (typically ~10 nm).³

The nanophase segregated morphology initially formed in P3HT/PCBM blends is a kinetically trapped, non-equilibrium state formed during spin-casting and evaporation of solvents below the glass transition T_g of the polymers. However, the immiscibility of components and tendency of crystallization has the potential to drive larger scale phase segregation and discontinuity of the binary structures. This process, exacerbated under the constant flux of thermal energy generated by solar irradiation, is thought to be a significant cause of a reduction in the D–A interfacial area and a degradation in power conversion efficiencies.⁴ To achieve durable organic photovoltaics, the nanometer-scaled morphology of the BHJ device must be preserved.⁵ In an attempt to accomplish a stable morphology,

*Corresponding author. E-mail: holdcroft@sfu.ca. Fax: +1 7787823765.

- (1) (a) Jenekhe, S. A.; Chen, X. L. *Science* **1998**, *279*, 1903. (b) Klok, H. A.; Lecommandoux, S. *Adv. Mater.* **2001**, *13*, 1217. (c) Benanti, T. L.; Venkataraman, D. *Photosynth. Res.* **2006**, *87*, 73. (d) Coakley, K. M.; McGehee, M. D. *Chem. Mater.* **2004**, *16*, 4533. (e) Gunes, S.; Neugebauer, H.; Sariciftci, N. S. *Chem. Rev.* **2007**, *107*, 1324. (f) Hoppe, H.; Sariciftci, N. S. *J. Mater. Res.* **2004**, *19*, 1924. (g) Thompson, B. C.; Fréchet, J. M. J. *Angew. Chem., Int. Ed.* **2008**, *47*, 58. (2) (a) Sivula, K.; Luscombe, C. K.; Thompson, B. C.; Fréchet, J. M. J. *J. Am. Chem. Soc.* **2006**, *128*, 13988. (b) Sivula, K.; Ball, Z. T.; Watanabe, N.; Fréchet, J. M. J. *Adv. Mater.* **2006**, *18*, 206. (c) Ma, W. L.; Yang, C. Y.; Gong, X.; Lee, K.; Heeger, A. J. *Adv. Funct. Mater.* **2005**, *15*, 1617. (d) Li, G.; Shrotriya, V.; Huang, J. S.; Yao, Y.; Moriarty, T.; Emery, K.; Yang, Y. *Nat. Mater.* **2005**, *4*, 864. (e) Reyes-Reyes, M.; Kim, K.; Carroll, D. L. *Appl. Phys. Lett.* **2005**, *87*, 83506. (f) Nishizawa, T.; Tajima, K.; Hashimoto, K. *J. Mater. Chem.* **2007**, *23*, 2440. (g) Liang, Y.; Xu, Z.; J. Xia, J.; Tsai, S. -T.; Wu, Y.; Li, G.; Ray, C.; Yu, L. *Adv. Mater.* **2010**, *22*, E135. (h) Banishoeib, F.; Adriaensens, P.; Berson, S.; Guillerez, S.; Douheret, O.; Manca, J.; Fourier, S.; Cleij, T. J.; Lutsen, L.; Vandezande, D. *Sol. Energy Mater. Sol. Cells* **2007**, *91*, 1026.

- (3) Shaw, P. E.; Ruseckas, A.; Samuel, I. D. W. *Adv. Mater.* **2008**, *20*, 3516. (4) Woo, C. H.; Thompson, B. C.; Kim, B. J.; Toney, M. F.; Fréchet, J. M. J. *J. Am. Chem. Soc.* **2008**, *130*, 16324. (5) (a) Miyanishi, S.; Tajima, K.; Hashimoto, K. *Macromolecules* **2009**, *42*, 1610. (b) Kim, B. J.; Miyamoto, Y.; Biwu Ma, B.; Fréchet, J. M. J. *Adv. Funct. Mater.* **2009**, *19*, 2273. (c) Helgesen, M.; Gevorgyan, S. A.; Krebs, F. C.; Janssen, R. A. J. *Chem. Mater.* **2009**, *21*, 4669. (d) Helgesen, M.; Krebs, F. C. *Macromolecules* **2010**, *43*, 1253.

thermocleavable materials have been applied as the active layer in organic PV devices.^{5c} These are solution processed but become insoluble after a thermal treatment providing a better operational stability for the devices.^{5d} This strategy has the potential to be applied in organic tandem PV or hybrid solar cells.⁶ We previously reported a similar approach in which fullerenes are covalently bonded to the polymer backbone.⁷ While it was shown that this approach was synthetically successful, that polymers containing a relatively high mass content of fullerene could be obtained, grafting fullerene-bearing side chains directly to P3HT was found to reduce the semicrystallinity of the P3HT domains, reduce the hole charge mobility, and significantly reduce their photovoltaic activity. This was caused by the much poorer solubility of the fullerene units relative to the polymer chains which aggregate during film casting and restrict self-organization of the conjugated polymer.⁷

In a recent study, morphological stabilization of polymer thin film was examined using a thermally cross-linkable poly(3-(5-hexenyl)thiophene).^{5a} A similar idea was explored using a series of photocross-linkable polythiophenes.^{5b} Both studies showed that deterioration of the photoconversion efficiency of polymer PV cells was partially suppressed.

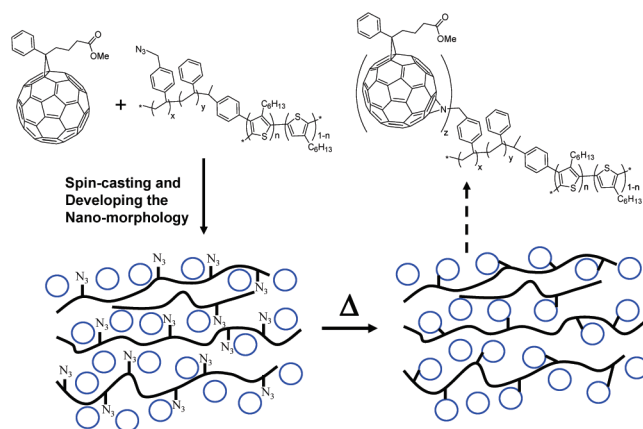
In the above studies, morphological stabilization is induced as a result of cross-linkability of a functionalized polymer. In the present study, we explore a slightly different strategy in which a chemical linkage between the donor polymer and the acceptor is formed, in order to minimize the impact of the acceptor on the organization of the donor polymer and at the same time stabilize the desired morphology. The strategy is demonstrated with a blend of an azide-functionalized graft copolymer and PCBM. It is anticipated that the azido-functionalized P3HT will self-organize into a nanoscopic domain forming a bicontinuous morphology with PCBM. Following this, a thermal treatment initiates covalent attachment of the polymer to PCBM, “locking-in” preformed domains. This process is shown schematically in Scheme 1.

Experimental Section

Materials. PCBM (>99.5% purity) was purchased from American Dye Source Inc. Styrene, ST (>99%) and 4-chloromethylstyrene, CMS (90%, Aldrich) were distilled under reduced pressure prior to use. 1,2-Dichlorobenzene (1,2-DCB, 99%, Aldrich) was distilled over anhydrous CaCl₂ under reduced pressure. P3HT (for fabrication of reference PV devices) was purchased from Reike Metals (regioregularity 90–93%).

Instrumentation and Procedures. A 500 MHz Bruker AVANCE III spectrometer was used to obtain ¹H NMR spectra in CDCl₃. Gel permeation chromatography (GPC) was performed using tetrahydrofuran (THF; HPLC grade from CALEDON Laboratories; flow rate of 1 mL/min at 165 psi and room temperature) on a Waters 1515 Isocratic HPLC pump with Waters 2414 refractive index and Waters 2487 absorbance

Scheme 1. Stabilization of the Nanomorphology by Solid State Reaction of PCBM with Azide-Functionalized Conjugated Polymer

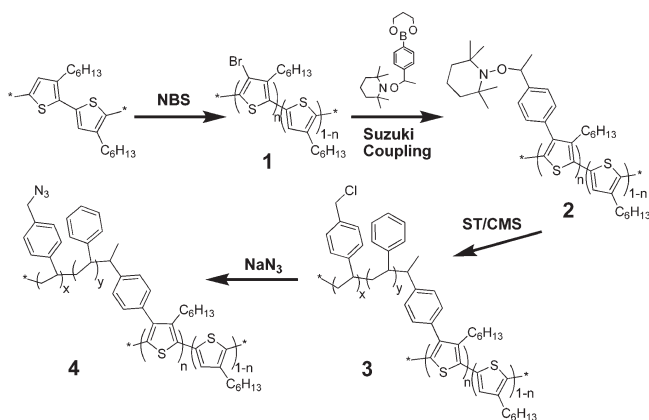


detectors against a polystyrene standard mixture composed of 2.9, 37, 110, and 390 KDa molecular weights. Absorption spectra were recorded on a Cary 3E spectrometer. Fourier transform infrared spectroscopy (FTIR) spectra were recorded using an ABB FTLA2000 system on samples diluted with KBr and pressed to make 1 cm disks. Bright-field transmission electron microscopy (TEM) images were recorded using a Hitachi 8100 system. Films, on poly(ethylene dioxythiophene)-polystyrene sulfonic acid (PEDOT-PSS)/glass substrate, were spin-cast at 1000 rpm from 1,2-DCB and left in a covered Petri dish to allow the solvent to evaporate slowly. Thermal annealing was performed on a hot plate at 150 °C in a glovebox. The films were then floated onto water and placed on a 500-mesh TEM copper grid. An optical microscope Nikon Eclipse 50i (equipped with a QICAM FAST 1394 camera) was also used to examine the active layer morphology when the surface features were > 2 μm. Current–voltage (*J–V*) measurements of devices were conducted on a computer-controlled Keithley 2400 Source Meter. A xenon lamp (300 W, 6258 Newport) equipped with a AM1.5G filter was used as the white light source. The optical power was 100 mW/cm², measured using a broadband power meter 841-PE (Newport) equipped with an Ophir thermal detector head (3A-P-SH-V1). The power was calibrated versus a Reference Solar Cell (91150 V Newport). The external quantum efficiency (EQE) was measured using monochromatic light from a Newport Cornerstone 260 monochromator, and the incident power was measured using a power/energy meter (Newport, 818-UV). PV devices were fabricated with the configuration, indium tin oxide (ITO)/PEDOT-PSS/BHJ blends/Al(Ca), on patterned and pre-cleaned ITO substrates. Stock solutions of azide-functionalized graft copolymer and PCBM (20 mg of the each) were prepared in 0.5 mL 1,2-DCB, stirred for 2 h at 40 °C, and filtered through a 0.45 μm PVDF membrane before they mixed. Different blend ratios were obtained by adding respective volume ratios of the stock solutions and stirring the mixture for 1 h. The blend mixture was spin-coated in a glovebox (O₂ and H₂O levels, <0.1 ppm) at a spin rate of 1000 rpm for 20 s preceded by two stages: 100 rpm (1 s) and 300 rpm (5 s). Spin-coated films were then left in a covered Petri dish to control the solvent evaporation rate (drying time: 20–40 min) and finally heated to 40 °C for 10 min on a hot plate. The cathode, Ca coated with Al, was thermally deposited through a shadow mask on the active layer using a Varian 3118 thermal evaporator. The active area of the device was 0.2 cm² adjusted through a shadow mask. The active layer thickness was ~150 nm while the PEDOT-PSS layer

(6) (a) Ameri, T.; Dennler, G.; Lungenschmied, C.; Brabec, C. J. *Energy Environ. Sci.* **2009**, *2*, 347. (b) Helgesen, M.; Søndergaard, R.; Krebs, F. C. *J. Mater. Chem.* **2010**, *20*, 36.

(7) (a) Chen, X.; Gholamkhash, B.; Han, X.; Vamvounis, G.; Holdcroft, S. *Macromol. Rapid Commun.* **2007**, *28*, 1792. (b) Gholamkhash, B.; Peckham, T. J.; Holdcroft, S. *Polym. Chem.* **2010**, *1*, 708.

Scheme 2. Synthetic Route to Azide-Functionalized Graft Copolymer 4 Possessing a Graft-Chain Density of 1% ($n = 0.01$)



(spin coated at 5000 rpm and baked at 140 °C for 10 min under ambient atmosphere) and Ca and Al thicknesses were typically 40, 20, and 80 nm, respectively, measured using an Alpha-Step IQ profilometer (KLA-Tencor). Although devices were stored in the glovebox until measurement, they were exposed to the atmosphere when transferred from the thermal evaporator to the glovebox. Fabricated devices were placed in a home-built holder under vacuum for J - V and EQE measurements.

Synthesis. The general synthetic procedures for the synthesis of macroinitiators and graft polymers are given below, and a summary is depicted in Scheme 2.

Poly-3-bromo-4-hexylthiophene, (1). *N*-Bromosuccinimide (0.01 equivalent) was added to a solution of P3HT in CHCl₃ under nitrogen. The mixture was stirred at room temperature overnight in the absence of light. The reaction mixture was heated to 50 °C for 2 h after which it was cooled to room temperature and washed with saturated NaHCO₃ solution and brine. After separation of the organic layer, the aqueous layer was further extracted with CHCl₃ and the combined organic layers were dried over MgSO₄. The concentrated mixture was poured into methanol and filtered, giving the target compound as a deep violet solid. The crude product was purified by Soxhlet extraction using MeOH and hexane sequentially. The CHCl₃ extract was concentrated, poured into methanol, and centrifuged. The precipitate was washed with MeOH and vacuum-dried. A detailed synthetic procedure for poly-3-bromo-4-hexylthiophene (1 mol % Br) **1a** is previously reported.^{7b}

Tempo(1%)-P3HT Macroinitiator (2). The synthesis of the tempo-styrene boronic ester, i.e., 1-[4-(4'-trimethylene-1,3,2-dioxaborolan-2-yl)phenyl]-1-(2,2,6,6-tetramethyl-1-piperidinyloxy)ethane from 1-(4'-bromophenyl)-1-(2'',2'',6'',6''-tetramethyl-1-piperidinyloxy)ethyl was described previously.^{7b} Briefly, partially brominated, poly(3-bromo-4-hexylthiophene) (**1**), tempo-styrene boronic ester and Pd(PPh₃)₄ were dissolved in THF and degassed by three freeze-pump-thaw cycles. Under a flow of nitrogen, a degassed solution of K₂CO₃ (0.2 mmol) in water was added to this mixture through a cannula. The reaction mixture was heated at 60 °C for 2 days under nitrogen after which it was concentrated. The concentrate was poured into MeOH, centrifuged, and washed several times with MeOH. The crude precipitate was dissolved in CHCl₃ and filtered through a column of alumina. The dark purple product was reprecipitated upon addition of the concentrate to MeOH, centrifuged, washed several times with MeOH, and dried at 50 °C under vacuum. A detailed synthetic procedure for **2** is previously reported.^{7b}

P3HT-1%graft-(ST-*stat*-CMS) (3). A mixture of tempo($n\%$)-P3HT (~40 mg) (**2**), styrene (2 mL), and CMS (1.25 mL) was purged with nitrogen for 20 min before stirring at 100 °C for 1 h. The product was poured into MeOH and centrifuged. The crude product was dissolved in CHCl₃ and loaded on a silica gel column. Flash chromatography was performed to remove the styrene homopolymer using an increasing solvent gradient of acetone in MeOH (from 20 to 50 and 100% to remove residual monomers) followed by CHCl₃ in acetone (from 10 to 20, 40, and 80% to remove oligomers and/or copolymers of ST/CMS). Finally, the product was eluted with CHCl₃, and the concentrate was poured into MeOH. The product was centrifuged, washed with MeOH, and vacuum-dried. A detailed synthetic procedure for **3** is previously reported.^{7b}

P3HT-1%graft-(ST-*stat*-N₃MS) (4) (where N₃MS denotes azidomethylstyrene). To a solution of **3** (~100 mg in 70 mL of chlorobenzene) was added excess amounts (4 equivalents) of sodium azide in DMF (30 mL). The mixture was heated to 100 °C for 3 h under nitrogen. After cooling to room temperature, the mixture was poured into MeOH (200 mL) and stirred. The precipitate was centrifuged, washed with MeOH/H₂O (4:1 v/v) and MeOH sequentially, and vacuum-dried. The product, if needed, was further purified by Soxhlet extraction using MeOH and hexane sequentially. A detailed synthetic procedure for **4** is previously reported.^{7b}

Results and Discussion

Synthetic Aspects. The synthetic approach to obtain a postfunctionalized P3HT with side chains consisting of a statistical polymer of CMS and ST is depicted in Scheme 2, and the details are reported elsewhere.⁷ Regioregular, head-to-tail (HT) P3HT was synthesized using the GRIM method.⁸ The HT regioregularity was found to be > 98%, as determined by the ¹H NMR. The number average (M_n) and weight average (M_w) molecular weights and polydispersity index (PDI) were estimated to be 27.9 KDa, 42.7 KDa, and 1.53, respectively, on the basis of GPC analysis. The degree of polymerization (DP) of P3HT is estimated to be 168. This sample was used to synthesize partially brominated P3HT (**1**), the tempo(1%)-P3HT macroinitiator (**2**), the precursor P3HT-1%graft-(ST-*stat*-CMS) (**3**), and the azide functionalized P3HT-1%graft-(ST-*stat*-N₃MS) (**4**).

Following a nitroxide-mediated radical polymerization (NMRP) of a statistical mixture of CMS and ST (feed ratio 34:66 wt %), a new set of broad signals at 7.0–7.2, 6.3–6.7, and 4.4–4.6 ppm emerged in the ¹H NMR spectra, attributed to phenyl and chloromethylene protons associated with the CMS/ST side chains. In the case of **3**, M_n (and M_w) increased to 28.3 (and 45.4) KDa, indicative of CMS/ST side-chain growth at the 4-position on the thieryl ring. The chlorine atoms in **3** were quantitatively substituted by azide groups to form the azido-functionalized polymer, **4**. The substitution reaction was monitored by NMR spectroscopy: for **3**, the broad peak of the methylene groups adjacent to Cl was observed at 4.5 ppm while, in the azido-containing polymer **4**, this peak is shifted to 4.2 ppm. Other protons exhibited the

(8) Loewe, R. S.; Ewbank, P. C.; Liu, J.; Zhai, L.; McCullough, R. D. *Macromolecules* **2001**, *34*, 4324.

Table 1. Graft Copolymer Compositions

compound	n^a (%)	DP of CMS ^b	DP of ST ^c	P3HT to side chain ^d (wt%)
3	1	30	50	74:26
4	1	32	50	84:16

^aDegree of postfunctionalization of P3HT (i.e., graft-chain density).

^bDegree of polymerization calculated from the integral of the 4.2/4.5 ppm peak per unit thienyl ring. ^cFrom the integral of the 6.5 ppm peak per unit thienyl. ^dBased on M_n for P3HT (GPC result: $M_n = 27.9$ KDa).

same chemical shifts. Following the conversion to the azide form, in the case of **4**, M_n (28.8 KDa) was found to be relatively unchanged to that of **3**.

The mole fraction of CMS/ST in the graft copolymers was determined using ¹H NMR integration of peaks at 4.5 (4.2 in the azide form), 6.5, and 2.78 ppm which correspond to CMS, ST + CMS, and α -methylene protons of P3HT moieties, respectively, of the graft copolymers. In order to maintain a high content of the active component, namely, the polythiophene backbone in the graft copolymer, and to maintain the optical and electronic properties of the native P3HT, relatively short length side chains of ST and CMS were grown on the macro-initiator by the NMRP reaction. Copolymer **3** was found to be composed of CMS/ST/P3HT with mole fractions of 0.2:0.3:1.0. Table 1 summarizes the degree of polymerization for CMS and ST and the mass percentage of polythiophene backbone to the CMS/ST side chains.

The cycloaddition of the azide group to PCBM was performed in the solid state after spin-coating a blend of copolymer **4** and PCBM. (See Scheme 1.) FTIR spectroscopy confirmed the cycloaddition reaction between the azide and PCBM. Figure 1 depicts the FTIR spectra of thin films of graft copolymer **4** and its blend with PCBM before and after solid state reaction at 150 °C. The spectra show the presence of the thiophene ring vibration and asymmetric C=C ring stretching at 3054 and 1508 cm⁻¹, respectively, as well as signatures of aliphatic side chains (asymmetric C-H stretching of -CH₃ and -CH₂- at 2955 and 2925 cm⁻¹, respectively, and symmetric stretching of -CH₂- at 2856 cm⁻¹). After treatment reaction at 150 °C, the intensity of the peak at 2095 cm⁻¹, attributed to the azide functional groups, is greatly reduced, indicative of the reaction of N₃. In contrast, heating film of the polymer **4** in the absence of PCBM showed very little decrease of the N₃ signal.

Optical Properties. The UV-vis absorption spectra of blends of films of copolymer **4** with PCBM, before and after solid state reaction are shown in Figure 2. The absorption spectra provide evidence of extensive π - π stacking of the polythiophene backbone, as indicated by absorption peaks at \sim 515, 550, and 600 nm and an extension of the π - π^* absorption band to 650 nm.⁹ Upon reaction at 150 °C for 1 h, the absorption spectra decrease in intensity slightly but remain largely unchanged. Upon washing the film with CHCl₃ to dissolve any soluble portions of the film after reaction, the active layer thickness

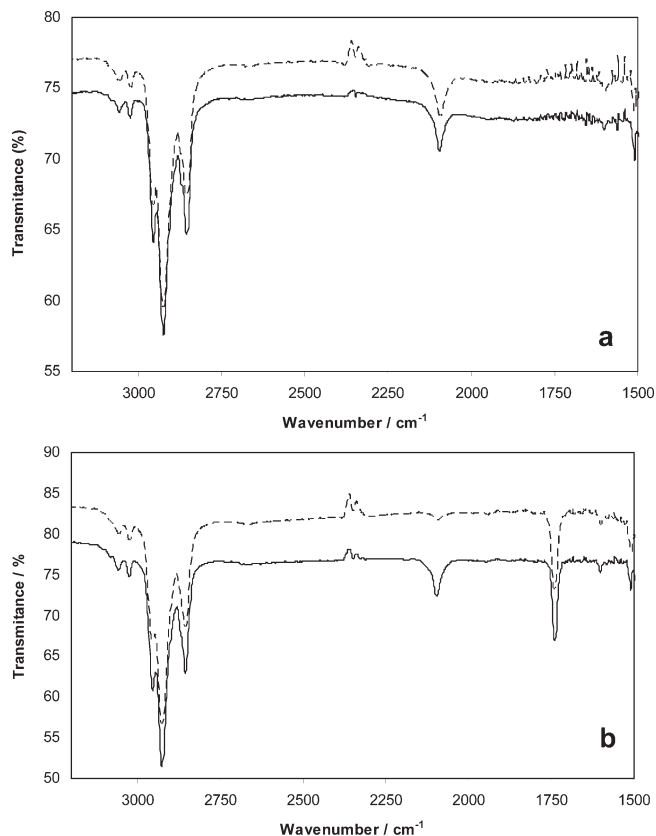


Figure 1. FTIR spectra of the graft copolymer **4** (a) and its 50:50 wt % blend with PCBM (b) before (solid) and after (dashed) treatment at 150 °C.

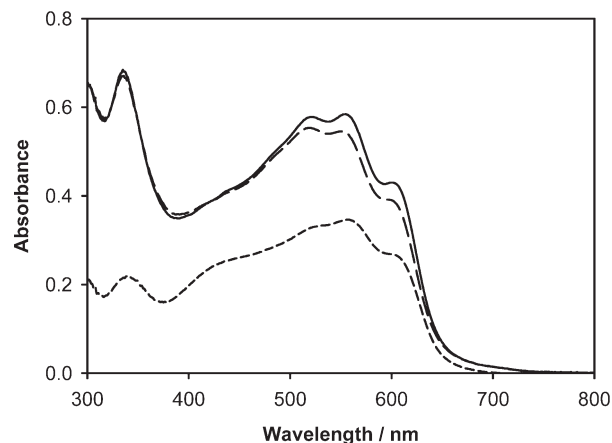


Figure 2. Absorption spectra of as-cast film of **4**/PCBM (50:50; solid line), after thermal treatment at 150 °C (1 h; long dash), and after washing in CHCl₃ (short dash).

is reduced from its initial value of 140 ± 10 to 100 nm. Accordingly, the absorption peak at 552 nm, attributed to **4**, decreases from 0.58 to 0.35, while that of PCBM, at 333 nm, decreases from 0.68 to 0.21, indicating \sim 60 and 30% of **4** and PCBM, respectively, remaining after washing. In contrast, unreacted blends of **4** and PCBM are completely dissolved with washing (not shown).

Morphology. Optical micrographs of **4**/PCBM and P3HT/PCBM (50:50) blends before and after 1 h of thermal treatment at 150 °C are shown in Figure 3. The micrographs of the P3HT/PCBM blend illustrates that

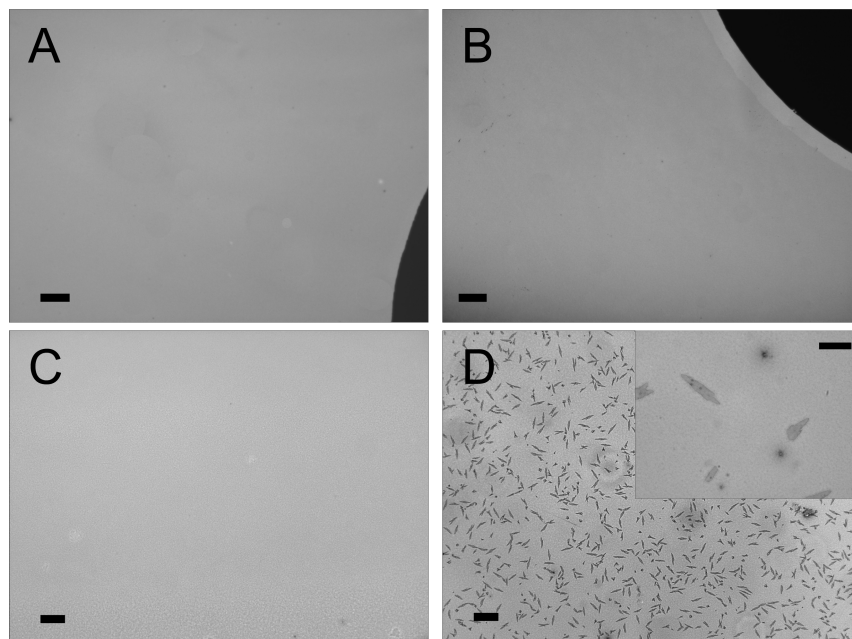


Figure 3. Optical micrographs of 4/PCBM blend (50:50) before (A) and after (B) 1 h treatment at 150 °C and of P3HT/PCBM (50:50) blend before (C) and after (D) thermal treatment (1 h at 150 °C). Scale bar = 100 μm . The inset in D shows an expanded view (scale bar, 8 μm).

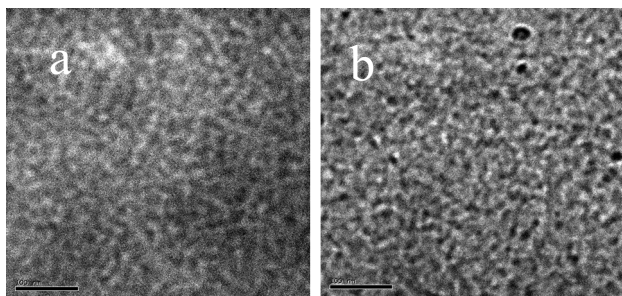


Figure 4. TEM images of the thin films of 4/PCBM before (a) and after (b) thermal annealing at 150 °C for 1 h. Scale bar, 100 nm.

thermal annealing induces the formation of needle-shape crystals of PCBM tens of micrometers in length, whereas in the case of 4/PCBM blends the formation of needle-shaped PCBM crystals is suppressed and the morphology stabilized due to the reaction between the azide-functionalized copolymer with PCBM.

Bright-field TEM images of a blend of the copolymer 4 and PCBM are shown in Figure 4. The micrograph of the as-cast films show evidence of a bicontinuous network of donor (dark) and acceptor (light) domains having feature sizes of 10–20 nm. After thermal treatment at 150 °C for 1 h, during which solid state reaction occurs, the morphology and corresponding domain sizes are unchanged. However, we also find that after the same thermal treatment TEM analysis indicates the nanoscale morphology of P3HT/PCBM blends are also unchanged (not shown). This indicates, surprisingly, that morphological analysis of nanophase segregation of BHJ films by TEM analysis does not necessary reveal the changes in component distribution that are observed under lower magnification.

Photovoltaic Properties. The PV activity of copolymer 4 blended with various mass ratios of PCBM was investigated.

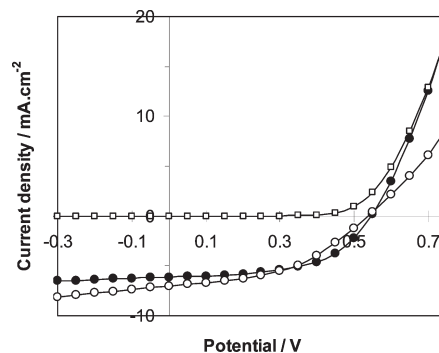


Figure 5. *IV* characteristics of 4/PCBM (40:60 w/w): as-cast (●), thermally reacted (○), and dark current (□).

PV devices were fabricated by spin-coating blends of the azide-functionalized copolymer and PCBM as well as P3HT/PCBM as reference devices. For the graft copolymer 4/PCBM devices, the best performance was obtained when the thermal annealing precedes the deposition of the cathode (Ca/Al). Furthermore, to optimize the wt% ratio for the graft copolymer and PCBM, PV devices with different blend ratios were fabricated. The best performance was observed for a device with 40:60 wt % blend ratio.

IV characteristics of devices prepared using as-cast and thermally reacted blends having a 40:60 wt % blend ratio (4/PCBM) are shown in Figure 5. The open circuit voltage (V_{oc}) for the as-cast and thermally reacted films is 0.55 V. This observation indicates that thermal reaction of the film does not modify the metal/blend interface, nor does it affect the ionization potential of the donor polymer or the electron affinity of the acceptor PCBM. The short-circuit current density (J_{sc}) increased from 6.15 to 7.01 mA/cm² following the annealing, indicating an improved efficiency of capturing of excitons. In contrast, the fill factor (FF) reduced from 0.55 to 0.45. The decrease in FF

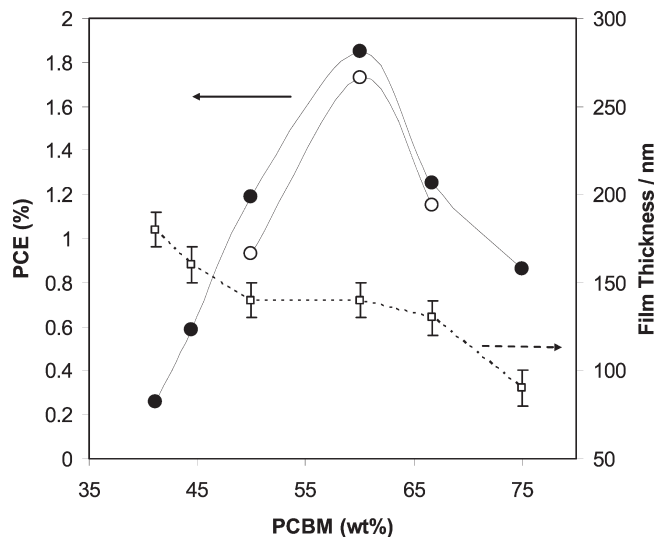


Figure 6. PCE as a function of blend ratio for **4**/PCBM devices; as-cast (●) and thermally annealed at 150 °C for 1 h (○). Film thicknesses (□) were measured after thermal treatment.

reveals the importance of series resistance and possibly a change in charge mobility across the active layer.¹⁰

Power conversion efficiencies (PCE) for PV devices prepared with varying ratios of **4**/PCBM are plotted in Figure 6. The maximum power was found for 40:60 wt % blends, with thermally reacted blends showing slightly lower PCEs for a given blend ratio. The initial maximum PCE for the thermally reacted films was 1.73%. This is lower than devices prepared using native P3HT/PCBM (50:50 w/w) blends prepared in our laboratory (2.5%) measured under the same conditions, which is an expected result based on the fact that the polythiophene content in copolymers **4** is ~84 wt % (see Table 1) and, thus, only ~33% in a 40:60 w/wt blend, i.e., much lower than the 50 wt % in native P3HT/PCBM blends.

Devices incorporating **4**/PCBM blends were subjected to accelerated lifetime testing by subjecting them to 150 °C for extended periods. The decrease in PCE as a function of time is shown in Figure 7. Despite beginning-of-life PCEs for **4**/PCBM blend devices being lower than native P3HT/PCBM blends, the rate of degradation of performance is slower, decreasing by only 50% over a 3 h period (compared to 80% for P3HT/PCBM films). We attribute this to partial stabilization of the morphology of the active layer due to the reaction between the azide functional groups of **4** with PCBM. However, the result is not entirely satisfactory, as evidenced by the partial loss in performance in time of **4**/PCBM devices. There are likely

(10) Neugebauer, H.; Brabec, C.; Hummelen, J. C.; Sariciftci, N. S. *Sol. Energy Mater. Sol. Cells* **2000**, *61*, 35.

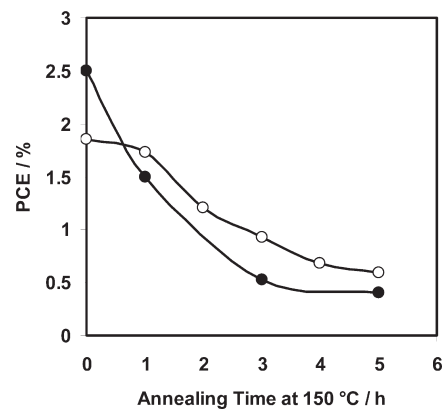


Figure 7. PCE as a function of annealing time for the P3HT/PCBM (●) and **4**/PCBM devices with 40:60 (○) wt% ratios.

other processes that undermine PV performance over time, such as interfacial degradation, delamination, oxidation, and chemical reactions at the metal electrode/organic interface.¹¹ Recent studies of organic PV devices have shown that the device instability may be related exposure to air/moisture. For example, an increased resistance at the PEDOT/PSS/blend layer interfaces is observed after air exposure due to a reduction in charge mobility and hole injection rate.¹² Measures to eliminate these and other degradation pathways are currently being pursued.

Conclusions

In this work, a series of postfunctionalized P3HT copolymers bearing a low graft-chain density (1%) of azide functionality was studied. These polymers were blended with PCBM, and the azide functionality was used to stabilize the bicontinuous D–A network formed through a cycloaddition reaction with PCBM. This prevented the growth of micrometer scale crystallites of PCBM that typically form over time. This approach reduced the rate of degradation of the PV performance over time, as evidenced by accelerated thermal testing. However, this strategy did not completely suppress degradation which implies other degradation pathways are present.

Acknowledgment. This work was supported through the NRC-NSERC-BDC Nanotechnology Initiative (NNBNI).

- (11) (a) Reese, M. O.; Morfa, A. J.; White, M. S.; Kopidakis, N.; Shaheen, S. E.; Rumbles, G.; Ginley, D. S. *Sol. Energy Mater. Sol. Cells* **2008**, *92*, 746. (b) Burrows, P. E.; Bulovic, V.; Forrest, S. R.; Sapochak, L. S.; McCarty, D. M.; Thompson, M. E. *Appl. Phys. Lett.* **1994**, *65*, 2922.
- (12) Kawano, K.; Pacios, R.; Poplavskyy, D.; Nelson, J.; Bradley, D. D. C.; Durrant, J. R. *Sol. Energy Mater. Sol. Cells* **2006**, *90*, 3520.